Assessment Supporting the Use of Outcropping Rock, Evolutionary Intensity Measures for Prediction of Liquefaction Consequences on Structures

Zach Bullock, Shideh Dashti, Abbie B. Liel, Keith A. Porter, Zana Karimi

ABSTRACT

This study evaluates a variety of intensity measures (IMs) for predicting the liquefaction-induced residual settlement and tilt of shallow-founded structures. We use data from both numerical and physical (centrifuge) models of soil-foundation-structure systems. The relative quality of these IMs is quantified in terms of efficiency, sufficiency, and predictability. We consider both scalar and vector-valued IMs and evaluate the relative performance of IMs recorded at different locations (outcropping rock, within rock, far-field, and foundation) from nonlinear and equivalent-linear simulations. Cumulative absolute velocity (CAV) at outcropping rock is the optimum IM for predicting foundation settlement, while either outcropping rock CAV, peak ground velocity, or peak incremental ground velocity is optimum for predicting permanent foundation tilt. Vector IMs offer improvements to efficiency and sufficiency, but may be impractical to predict.

INTRODUCTION

The first step in performance-based structural and geotechnical earthquake engineering after one identifies the asset under consideration involves the selection of intensity measures (IMs). Ground motion intensity is a key component in any model for predicting consequences of earthquakes and, often, uncertainty around ground motion intensity is the largest component of the total uncertainty in a prediction (e.g., Bray and Travasarou 2007; Bray and Macedo 2017). In this study, we evaluate a wide variety of IMs for predicting earthquake-induced settlement and tilt of shallow-founded structures on liquefiable ground. Settlement and tilt are referred to as demand parameters (DPs). Careful IM selection is critical to the quality of predictive models, and can reduce modeling uncertainty and ensure practicality. The IMs considered here vary in terms of how the intensity is quantified (i.e., considering evolutionary parameters, which depend on the amplitude, duration, and frequency content of motion, and

peak parameters, which depend on the amplitude and sometimes frequency content of motion, but not duration), the location at which that intensity is measured (i.e., at bedrock below a soil column, rock outcrop, far-field soil surface, or the foundation), and the type of analysis used to estimate an IM value (i.e., 1D equivalent-linear analyses, 3D nonlinear, fully-coupled simulations, etc.). Thus, this study considers a thorough selection of IMs as measured according to a variety of analyses to identify the optimum IMs for predicting foundation settlement and tilt due to earthquake-induced liquefaction.

BACKGROUND

Many studies have evaluated the quality of various IMs for predicting structural and geotechnical DPs (e.g., Shome and Cornell 1999; Luco and Cornell 2007; Padgett et al. 2008). Luco and Cornell (2007) formally defined the quality of an IM for predicting a DP in terms of "efficiency" and "sufficiency." An efficient IM results in relatively small variability around its predictions of the DP in question and, therefore, smaller uncertainty in probabilistic predictive models. A sufficient IM results in predictions of DP that are unbiased on all earthquake source, path, and site parameters that affect the IM. In the context of developing predictive models for DPs, the availability and efficiency of ground motion models (GMMs) for predicting a given IM is also important, which is termed "predictability." Unpredictable IMs are impractical to use for forward analysis, regardless of their efficiency and sufficiency.

Existing procedures have identified the usefulness of evolutionary IMs for predicting geotechnical consequences of earthquakes: Kramer and Mitchell (2006) using cumulative absolute velocity (CAV) above a 5 cm/s^2 threshold (CAV_5) for liquefaction triggering; Bray and Macedo (2017) using damage potential CAV (CAV_{DP}) for predicting settlement of shallow foundations on liquefiable ground; and Bullock et al. (2018a) using CAV for predicting settlement of shallow foundations on liquefiable ground. One of these studies also employed vector IMs containing peak transient and evolutionary IMs (Bray and Macedo 2017). Evolutionary IMs are somewhat less common in structural engineering, although some studies have highlighted their applicability (e.g., Kayen and Mitchell 1977). Structural engineers have also employed vector IMs including peak ground acceleration (PGA), peak ground velocity (PGV), or spectral acceleration (S_a) in combination with a measure of duration (e.g., Bommer et al. 2004; Raghunandan and Liel 2013; Chandramohan et al. 2016).

Most procedures related to liquefaction triggering and consequences (e.g., Youd and Idriss 2001; Cetin et al. 2009; Unutmaz and Cetin 2012; Boulanger and Idriss 2014) use the cyclic stress ratio (CSR) as a measure of intensity, which is a function of soil surface peak ground acceleration (PGA) at a hypothetical far-field location, typically obtained from 1D, equivalent-linear, total-stress site response analyses. CSR is sometimes adjusted to incorporate the presence of the building (e.g., Cetin et al. 2009; Unutmaz and Cetin 2012). These procedures also often indirectly consider the influence of duration by including the earthquake's moment magnitude (M_W). To select a more optimum IM, Karimi and Dashti (2017) and Bullock et al. (2018a) used a similar approach to Luco and Cornell (2007), concluding that outcropping rock CAV was optimum for predicting permanent average settlement of mat-founded structures on liquefiable soils, based on 3D, nonlinear, fully-coupled, dynamic numerical simulations. Note that the settlements observed in these numerical simulations primarily capture deviatoric-type deformations (Karimi et al. 2018; Bullock et al. 2018a). Also note that Bullock et al. (2018a) used the same, extensive numerical database as this study, but considered only a few IMs, evaluated only settlement and did not fully document the IM evaluation. In a separate study, Bray and Macedo (2017) used a vector far-field IM including CAV_{DP} and $S_a(1.0)$ to predict the deviatoric component of foundation settlement.

This study evaluates a wider variety of IMs than previous studies using a single set of quality metrics according to both numerical and centrifuge test results. Although insightful, prior studies often did not consider a comprehensive variety of IMs or the full range of methodologies or locations for their estimation. For instance, Karimi and Dashti (2017) did not consider IMs calculated using equivalent-linear analyses, used a less extensive numerical database than the present study (e.g., approximately 1,600 compared to more than 63,000 with additional variations in motion and system properties), did not differentiate between the outcropping rock and within-rock motion for predicting foundation settlement (because their simulations employed a rigid bedrock), and did not confirm their conclusions with experimental results. Additionally, the previous work did not consider whether certain IMs are better or worse in certain ranges of soil-foundation-structure parameters, which may influence IM selection in predictive models; did not consider vector IMs (i.e., using multiple IMs in one predictive model); and did not investigate the possible influence of rotational motion at the foundation. Therefore, these IM selections may not be optimum in terms of performance or predictability, and they need to be reevaluated more comprehensively and consistently at

different locations using different types of analyses common in practice, to evaluate both residual settlement and tilt of the foundation.

OBJECTIVE AND METHODS

Performance-based earthquake engineering (PBEE) requires probabilistic estimates of both IMs and DPs. We adopt a double integral version of the PBEE framework equations, i.e.:

$$\lambda(DM) = \iint G(DM|DP)dG(DP|IM)d\lambda(IM) \quad (1)$$

In this equation, $\lambda(\cdot)$ is the mean annual rate of exceedance of the argument, $G(\cdot)$ is the complementary cumulative distribution function of the argument, and DM is a damage measure. In this study, DMs would be represented by threshold values of the DPs (e.g., "excessive" settlement or residual tilt defined according to some limiting threshold). GMMs consisting of a rupture forecast (i.e., the location, geometry, magnitude, and rates of occurrence of relevant earthquakes; e.g., Field et al. 2015) and one or more ground motion prediction equations (e.g., Campbell and Bozorgnia 2014) provide the rate of occurrence of IM values ($d\lambda(IM)$) in this equation. The rate of occurrence of an IM (λ(IM)) plotted against the IM values is commonly referred to as the hazard curve. Structural and geotechnical models are used to probabilistically estimate DPs conditioned on IMs, denoted here as $dG(DP|IM)$.

In this study, we use both results of numerical analyses (nonlinear and equivalent-linear) and centrifuge experimental results to compare competing IMs for use in estimating settlement and residual tilt of mat-founded structures on liquefiable ground. We consider these datasets rather than observations of real buildings experiencing strong ground motion, settlement, and residual tilt because very few detailed recordings of motion or settlement are available, and those which are available include only ground motion recorded at the surface of a nearby far-field site, which may or may not reflect the soil profile and motions near the structure in question.

QUALITY METRICS

Efficiency, sufficiency, and predictability are common measures of the performance of IMs (e.g., Luco and Cornell 2007; Eads et al. 2015; Dashti and Karimi 2017). Efficiency is a measure of dispersion in the errors in prediction of DP based on IM: how accurately can an IM predict a DP with no other information? Sufficiency is a measure of bias in the errors on an

earthquake scenario's source, path, and site parameters (e.g., moment magnitude, M_W, or distance to rupture, R_{rup}): does an IM capture all relevant information in an earthquake record? Predictability is a measure of the practicality of generating probabilistic estimates of a given IM using ground motion models (GMMs): can we actually implement a model that uses a given IM, and what is the uncertainty in predicting the IM itself?

We formally define efficiency as the standard deviation of the logarithmic residuals ($\varepsilon_{DP|IM}$) of a regression between the IM and DP, according to Equation 2.

$$\ln(DP) = a_0 + a_1 \ln(IM) + \varepsilon_{DP|IM} \quad (2)$$

Previous studies considering efficiency and sufficiency (e.g., Luco and Cornell 2007) have opted to use the typical σ notation used for other standard deviations. However, to avoid confusion and to minimize the need for complex subscripts, we denote efficiency as $E_{DP} = \text{std}(\varepsilon_{DP|IM})$. E_{DP} is always positive, and smaller values reflect higher efficiency because there is less uncertainty around the predictions of the DP.

An IM is "sufficient" if its predictions are functionally independent from all earthquake parameters. Sufficiency is crucial because the PBEE framework equation (Equation 1) is only valid for sufficient IMs. Although sufficiency technically pertains to all earthquake scenario parameters including those pertaining to site effects and secondary effects such as hanging-wall effects, only the primary parameters of magnitude and distance are typically evaluated (e.g., Luco and Cornell 2007). These parameters are the most influential for the intensity of ground motion at a given location in a given earthquake (e.g., Abrahamson et al. 2013; Boore et al. 2014; Campbell and Bozorgnia 2014; Chiou and Youngs 2014). Here, we use the regressions in Equations 3 and 4 to quantify sufficiency with regard to magnitude and distance and the unexplained variation (residuals) from Equation 2.

$$\varepsilon_{DP|IM} = b_{0,M} + b_1 M_W + residual \quad (3)$$

$$\varepsilon_{DP|IM} = b_{0,R} + b_2 \ln(R_{rup}) + residual \quad (4)$$

We formally define sufficiency with regard to M_W or R_{rup}, denoted $S_{DP,M}$ or $S_{DP,R}$, respectively, according to Equations 5 and 6:

148 $$S_{DP,M} = \left|\frac{b_1[\max(M_W)-\min(M_W)]}{\max(\varepsilon_{DP|IM})-\min(\varepsilon_{DP|IM})}\right| \quad (5)$$

149 $$S_{DP,R} = \left|\frac{b_2[\max(\ln(R_{rup}))-\min(\ln(R_{rup}))]}{\max(\varepsilon_{DP|IM})-\min(\varepsilon_{DP|IM})}\right| \quad (6)$$

150 The numerators in these equations reflect the total change in estimated $\varepsilon_{DP|IM}$ over the total
151 range of M_W or R_{rup} considered, and the denominators are the total ranges of observed values
152 of $\varepsilon_{DP|IM}$. $S_{DP,M}$ and $S_{DP,R}$ therefore represent the portion of the total range of $\varepsilon_{DP|IM}$ that is
153 the result of bias on M_W or R_{rup}, and smaller values are desirable. Using this definition of
154 sufficiency allows us to directly compare the sufficiency of different IMs and DPs (each
155 combination of which will have a different range of $\varepsilon_{DP|IM}$, and also to compare the sufficiency
156 with respect to magnitude and that with respect to distance. We generally consider 5% to be an
157 upper bound on acceptable sufficiency defined this way, although we primarily consider the
158 relative sufficiency in this study. The 5% threshold is somewhat arbitrary, but aligns with the
159 use of 5% as a threshold elsewhere in statistics (e.g., the ubiquitous 5% significance level).

160 We quantify predictability as the uncertainty (i.e., the total standard deviation of
161 residuals, which we denote σ_p in this study) around the predictions of GMMs for a given IM.
162 However, the availability of GMMs for a wide variety of locations and tectonic environments
163 and the robustness of databases used to develop the GMMs should also be considered; even if
164 a very accurate GMM exists for a given IM, it is not considered predictable if that GMM is
165 limited in applicability.

166 Two additional metrics have been used in other IM studies: practicality and proficiency
167 (e.g., Padgett et al. 2008). Practicality is a measure of the strength of relationship between the
168 IM and DP, i.e. the value of the coefficient a_1 in Equation 2. Proficiency (ζ_{DP}) combines the
169 concepts of efficiency and practicality ($\zeta_{DP} = E_{DP}/a_1$) into a single metric. Appendix A
170 provides values for practicality and proficiency.

171 **DEFINITION AND LOCATION OF MOTION**

172 Before selecting specific IMs, we need to be very clear about what we mean by *motion* or a
173 *ground motion record*. Where is this motion occurring and which type of analysis is used to
174 obtain it? These questions have implications for the efficiency and sufficiency of IMs – is
175 motion at the surface of a nonlinear or equivalent-linear, liquefiable soil column a better

predictor of liquefaction consequences than the motion at its base? Motion location is also related to predictability; do models exist that are applicable for predicting a given IM at a particular location and what is the uncertainty associated with those models?

We consider the following five definitions of motion (Figure 1): outcropping rock motion (OR), within-rock motion (WR), far-field surface motion as estimated using 1D equivalent-linear site response analyses (FF-EL), far-field surface motion as estimated using 3D nonlinear dynamic analyses (FF-NL), and foundation motion as estimated using 3D nonlinear dynamic analyses of the soil-structure system (FN-NL). The motion at each location is the (horizontal) transverse acceleration recorded in the direction of shaking. These five definitions of motion each convey different information. The outcropping rock motion is the input motion to the more complex analyses and easiest to estimate for forward prediction with the lowest degree of uncertainty. IMs at this location are commonly used for selection of ground motion records in complex hazard analyses (e.g., Kramer and Mitchell 2006; Karimi et al. 2018). The within-rock motion is that recorded at the base of the soil column and is therefore influenced by the properties of the outcropping rock motion as well as the bedrock and soil above. The far-field motion is typically associated with liquefaction triggering analyses and forms the basis for many procedures (e.g., Cetin et al. 2009; Boulanger and Idriss 2014). We include the equivalent-linear far-field motion because these analyses are commonly used in practice to obtain surficial IMs based on the assumption of no liquefaction, and the nonlinear far-field motion because it is more likely to reflect the characteristics of motion above the liquefiable material. Equivalent-linear analyses are used, rather than nonlinear total-stress analyses, because they require less information to implement (and are therefore more practical and common) and because they are more distinct from the FF-NL motion. FF-NL is provided for comparison, but is not ideal from the perspective of practicality and simplicity in prediction of liquefaction consequences. Lastly, the motion at the foundation was expected to most closely link to certain deformation mechanisms, particularly those involving the generation of shear stresses and strains near the foundation (Dashti et al. 2010a,b). Therefore, even though impractical in terms of predictability, the foundation motion was considered among different locations for comparison of efficiency and sufficiency.

NUMERICAL MODELING OF SHALLOW-FOUNDED STRUCTURES

An extensive numerical study of shallow-founded structures on liquefiable ground provides the first dataset for this study (Karimi et al. 2018). That study employed 421 3D, solid-fluid, fully-coupled, effective stress, finite element simulations of soil-foundation-structure systems on layered, potentially-liquefiable ground, each analyzed under 150 ground motion records, producing approximately 63,000 total analyses that quantify ground motion intensity at various locations, as well as the demands on the foundation and structure. Figure 2 shows a schematic diagram of the models and provides a summary of the parameters that were varied. Appendix B provides additional details regarding these variations. These models used the PDMY02 soil constitutive model (Elgamal et al. 2002) with parameters calibrated according to cyclic shear and centrifuge tests (Karimi and Dashti 2015, 2016).

Karimi et al. (2018) used the fault-normal or maximum rotated horizontal component of ground motion as the one-directional input excitation for the models, applied parallel to the short side of the foundation. Outcropping rock motions were used as inputs to the numerical models, which were converted to within-rock motions using dashpots defined by the bedrock properties (Lysmer and Kuhlemeyer 1969). The input excitation was applied to the base nodes as a force time history derived from the bedrock density, the bedrock shear wave velocity, and the outcropping rock velocity time history. Equal-degree-of-freedom constraints were applied to all nodes at the boundaries, such that all boundary nodes at a given depth had the same motion. The foundation was tied directly to the soil, meaning the foundation was unable to slide relative to the neighboring soil.

For use of these results in this study, the far-field motion is recorded at a surficial location away from the foundation and away from the edge of the mesh to avoid boundary effects. The node selected to record the far-field motion was validated according to one-dimensional (1D, single column) analyses of the same soil profile. The foundation motion is the average transverse acceleration of the foundation's corners. We calculate settlement by taking the average of vertical displacements at each corner of the mat foundation, and we calculate residual tilt by dividing the differential settlement by foundation width in the direction of shaking. The applied excitation was 1D (horizontal) in these simulations, such that tilt always occurred in the direction of the foundation width, B (as opposed to its length, L).

This constitutive model and numerical modeling approach provide good predictions of foundation settlement (particularly for soil profiles with relatively thin liquefiable layers, where shear-type deformations are dominant), foundation acceleration demand, and pore pressure generation in the liquefiable material (Karimi and Dashti 2015, 2016). However, key limitations remain. In particular, these continuum models cannot capture certain deformation modes (e.g., sand ejection). In addition, the PDMY02 soil model may not accurately account for volumetric deformation modes, such as sedimentation, in a liquefied deposit. Further, the models may not accurately capture the influence of structure's inertia on residual tilt for a number of reasons. In particular, certain parameters (e.g., structure height and mass) that are correlated in the field were artificially separated in the parametric study. The model structures were idealized as elastic single-degree-of-freedom (SDOF) oscillators, and therefore did not include the influence of inelastic deformations in the structure or of vibration in multiple modes. Lastly, the foundation elements were attached to soil in these simulations (i.e., no interface models), limiting the extent and accumulation of inertial rocking and distortion around the foundation edges.

We also performed 1D equivalent-linear analyses using DeepSoil 6.1 (Hashash et al. 2016) to estimate the motion in the far-field for each distinct soil profile represented in the numerical database above. These analyses utilized the damping and shear modulus reduction curves proposed by Darendeli (2001), and shear wave velocity profiles were formulated according to Kramer (1996) and Jamiolkowski et al. (1991). The maximum shear strain observed at any point in a given profile ranged from 0% to 0.3% during different motions, with a 90^{th} percentile of 0.1%. These strains are mostly below the limit used for equivalent-linear analyses of approximately 0.3 to 0.5% (Stewart et al. 2014). Appendix C provides more details on the calculation of various parameters for the equivalent-linear analyses.

CENTRIFUGE TESTING

For further information on centrifuge modeling of soil liquefaction and its consequences on soil-structure interaction and building performance or centrifuge modeling of soil-structure interaction in general, please refer to Dashti (2009); Dashti et al. (2010a,b); Mason et al. (2013); Trombetta et al. (2013); Olarte et al. (2017, 2018); Paramasivam (2018a). Table 1 summarizes the database of centrifuge test results used in this study, and Appendix B provides additional details. We include only tests with flexible structures (as opposed to rigid blocks)

on shallow mat foundations. The results from centrifuge tests were critical during the validation and calibration of numerical models. These tests also provide data for the IM study that avoid certain limitations of numerical modeling. In particular, the physical models can partly capture ejection (due to homogeneous soil conditions) and all deformation modes (e.g., volumetric strains due to sedimentation). Despite the factors that may limit or reduce ejection in the centrifuge (mainly lack of inhomogeneity and spatial variations in permeability), it has been observed in several experiments (e.g., Fiegel and Kutter 1994; Paramasivam et al. 2018a,b; Badanagki et al. 2018).

Of course, centrifuge testing has its own set of limitations. For practical reasons, the same physical specimens are usually subjected to multiple sequential ground motions in the centrifuge. The first strong motion results in residual settlement and tilt of the foundation and densification of different soil layers (altering their geometry and properties). Subsequent tests on the same specimen therefore do not have the same initial conditions, and their results depend on the history of tests run during that spin of the centrifuge. In addition, centrifuge testing typically uses ground motion records that have been scaled and altered in frequency content to accommodate the shake table's capabilities. Once altered, ground motions may no longer realistically correspond to a real magnitude-distance scenario. Therefore, we can only use the results from centrifuge to evaluate efficiency, but not sufficiency. Lastly, although there is some variation in soil-foundation-structure system parameters in the available centrifuge data, there is not enough to consider parametric efficiency, which is subsequently discussed using the numerical database.

In interpreting centrifuge test results, we consider the outcropping rock and within-rock motion to be equal to the motion recorded at the base of the soil. For this case, the outcropping rock and within-rock motion are the same because the base of the container is relatively stiff (for infinitely stiff media, outcropping rock and within-rock motion are theoretically equivalent). The surficial far-field motion and the foundation motion for each structure were recorded using accelerometers in each test. The centrifuge tests also provide the opportunity to evaluate IMs in terms of a foundation's rotational acceleration, which may not be captured accurately in the numerical analyses because of constraints related to the lack of interface elements (Karimi and Dashti 2016). Rotational acceleration (in rad/s^2) is defined as the inverse sine of the difference in two vertical acceleration records at the edges of the foundation divided by their separation.

INTENSITY MEASURES CONSIDERED

The population of IMs considered in this study includes 11 peak transient IMs, 5 evolutionary IMs, and 4 duration-related IMs. We also consider vector-valued IMs consisting of one of the peak transient IMs paired with one of the evolutionary or duration-related IMs. These pairs are determined after examining the performance of the individual IMs. Table 2 summarizes these IMs and provides equations for their calculation. In these equations, t_d is the total duration of a given ground motion record, and $a(t)$ is its acceleration time history, $\chi\langle a(t)\rangle$ is a filter that is zero when $a(t)$ is below 5 cm/s^2 and one otherwise, $H(\cdot)$ is the Heaviside step function. CAV_{DP} is equal to CAV_{STD} if pseudo-spectral acceleration (S_a) exceeds $0.2g$ at any period between 0.1 and 0.5 sec, and pseudo-spectral velocity (S_v) exceeds 15.34 cm/s at any period between 0.5 and 1.0 sec, and zero otherwise.

We consider S_a at a handful of periods: 1.0 sec; the fixed-base fundamental period of the structure (T_{st}); the initial fundamental period of the site in the far-field (T_{so}); and lengthened versions of site period ($1.5T_{so}$ and $2T_{so}$). These lengthened site periods reflect the expectation that a liquefiable site will soften at larger shear strains during shaking. In addition to S_a, we include average pseudo-spectral acceleration ($S_{a,avg}$). $S_{a,avg}$ reflects the frequency content over a range of periods, and is therefore more effective than single-period values of S_a for predicting nonlinear structural response (e.g., Bianchini et al. 2009; De Biasio et al. 2014). This improvement in performance is due to the fact that: (1) structures have multiple modal periods, and (2) a structure's period changes as its strength and stiffness are altered by degradation during shaking, an effect which we also anticipate in soil columns. In the equation for $S_{a,avg}$, T_i are discrete periods used to represent the range from T_1 to T_2, and N is the number of discrete periods considered. We use 100 evenly spaced T_i ranging from T_1 to T_2. This equation uses T_1 and T_2 to arbitrarily represent the window of periods over which S_a is being averaged. Subsequently, various versions of $S_{a,avg}$ will be described with different values of T_1 and T_2 (e.g., $S_{a,avg}(0.2T_{so}, 1.5T_{so})$ for the average spectral acceleration over the period range from 20% to 150% of the initial site period).

EFFICIENCY AND SUFFICIENCY OF IMS FROM THE NUMERICAL DATABASE

First, we evaluate efficiency and sufficiency of all the considered IMs for settlement and tilt using the complete numerical database of all models and motions, describing this assessment

as "comprehensive" and labeled with a subscript C, i.e. $E_{DP,C}$, $S_{DP,M,C}$, and $S_{DP,R,C}$. If this data were used to create predictive relations of DPs with consistent IM(s), the comprehensive quality metrics would be directly linked to the final uncertainty and bias in those relations.

Second, we investigate the model-specific (or "parametric") efficiency and sufficiency of IMs as a function of various soil profile, foundation, or structure input parameters (e.g., foundation width, B, or foundation bearing pressure, q), denoted with a subscript P ($E_{DP,P}$, $S_{DP,M,P}$, and $S_{DP,R,P}$), because each is considered as a function of an input parameter. The parametric quality metrics allow us to identify situations in which certain IMs are more or less desirable, which might influence IM selection if an IM is poor in critical ranges of primary parameters. These values are calculated in the same manner as the comprehensive values, but using only the results from one specific model at a time (i.e., using analyses with all ground motions from one model, rather than all model-motion combinations together). By considering these values for a subset of models in which only one parameter was varied, we can observe the influence of a parameter on the efficiency and sufficiency of various IMs in isolation.

COMPREHENSIVE EVALUATION OF SINGLE IMS

We first consider the comprehensive efficiency and sufficiency of single IMs in predicting the permanent settlement of foundation (i.e., subscript S) in the numerical database. Recall that this settlement captures primarily the deviatoric-type deformations, but also partially captures volumetric deformations, mainly those resulting from partial drainage during shaking (Karimi et al. 2018; Bullock et al. 2018a). Figures 3 and 4 show efficiency (x-axis) and sufficiency (y-axis) for each IM. Recall that smaller values of $S_{S,M,C}$, $S_{S,R,C}$, and $E_{S,C}$ are better, so values plotted closer to the lower left are most sufficient and efficient. For values of efficiency and sufficiency of specific IMs, please refer to Tables A1 and A2 in Appendix A.

These figures show that evolutionary IMs perform consistently better than peak transient and duration-related IMs in terms of $E_{S,C}$ and $S_{S,M,C}$. The latter may be a result of these IMs incorporating effects of both the amplitude and duration of motion. Peak transient IMs generally have better sufficiency with respect to distance ($S_{S,R,C}$), but this depends on the location. In particular, S_a-based measures have relatively better $S_{S,R,C}$. The results also show that all IMs tend to be more sufficient with regard to distance than magnitude ($S_{S,R,C} = 0\%$ to 20% compared to $S_{S,M,C} = 0\%$ to 50%). The significant durations (D_{5-75} and D_{5-95}) are the

least efficient and sufficient regardless of location. However, we expect the duration measures to be more beneficial when paired with another amplitude-dependent IM.

Within each category of IM, the outcropping rock (OR) and within-rock (WR) motions are consistently more efficient and sufficient than the surficial motions. We hypothesize that this is because the OR and WR motions represent the seismic excitation applied to the entire system, where the surficial locations each only reflect a portion of that excitation (often highly de-amplified at higher frequencies due to wave propagation through a softened soil profile), which might therefore only provide good predictive capability of certain deformation modes. For example, volumetric deformations within thick liquefiable layers may not be well captured if only the de-amplified /modified nonlinear motion is used. The equivalent-linear far-field (FF-EL) location is more efficient and sufficient than the other surficial locations (FF-NL and FN-NL) for most IMs, because it incorporates vertical propagation of shear waves through the soil column without capturing strong soil nonlinearity, pore pressure generation, and the resulting de-amplification of high-frequency accelerations. Evolutionary IMs at the OR and WR locations are also more sufficient than peak transient IMs at the same locations with regard to distance.

Among single IMs, variants of CAV at the WR or OR locations offer the best combination of efficiency and sufficiency for predicting foundation settlement. Conversely, no single IM offers a clearly "optimum" combination of efficiency and sufficiency for residual tilt (figures provided in Appendix D). Vector IMs consisting of one evolutionary and one peak transient IM may be superior for predicting foundation tilt, and are explored in the next section.

COMPREHENSIVE EVALUATION OF VECTOR IMS

The analysis of the quality of single IMs suggests that a vector IM may improve the predictions of settlement and tilt. Here, Equation 2 is replaced with Equation 7 for calculating $\varepsilon_{DP|IM}$ to incorporate a second IM.

$$\ln(DP) = a_0 + a_1 \ln(IM_1) + a_2 \ln(IM_2) + \varepsilon_{DP|IM} \quad (7)$$

Table 3 reports the comprehensive efficiency and sufficiency of select pairs of IMs for predicting settlement. The combinations of IMs presented in the table were selected to show a representative variety (for instance, all variants of CAV have similar performance). For pairs

including an evolutionary IM and a peak transient IM, efficiency is not improved (up to 3% change) compared to more efficient individual IMs. However, for pairs including a duration measure, adding PGA or V_{gi} yielded better efficiency than either IM alone (up to 11% change). In particular, the efficiency of D_{5-75} and PGA or V_{gi} is similar to that of CAV alone. This suggests that CAV incorporates the effects of both the amplitude and duration of motion on foundation settlement.

As discussed above, evolutionary IMs are generally more sufficient with regard to magnitude and less sufficient with regard to distance than peak transient IMs. The IM pairs including one evolutionary and one peak transient IM are relatively sufficient with regard to both magnitude and distance ($S_{S,R,C}$ or $S_{S,M,C}$ <4%). Combining a duration measure with a peak transient IM also offers improved sufficiency compared to one or the other IM, but pairs including an evolutionary IM remain generally more sufficient. The results for predicting tilt in Appendix D are similar: pairs of IMs offer marginal improvements in efficiency and substantial improvements in sufficiency.

PARAMETRIC EVALUATION OF IMS

Although the comprehensive metrics of efficiency and sufficiency reflect the development of general procedures for estimating liquefaction consequences with broad applicability, there may be certain soil profiles, foundations, or structures in which different IMs are optimum.

Figure 5 shows $E_{S,P}$ as a function of three aspects of soil profile geometry: (a) the total deposit depth (H_{dep}), (b) the thickness of the liquefiable layer (H_L), and (c) the thickness of non-liquefiable crust at the surface (D_L). We select these parameters because H_L and D_L were identified as having critical influence on settlement in past studies (Karimi et al. 2018), and we expect H_{dep} to shed light on the choice between the base and surficial motions in predicting foundation settlement. Note that in this section, we exclude the within-rock motion, because it shows similar trends as the outcropping rock motion.

The efficiency of OR IMs is insensitive to H_{dep}. While the efficiency of IMs at surficial locations (i.e., FF-EL, FF-NL and FN-NL) improves for deeper deposits, they are still less efficient than the outcropping rock motion for even an 80 m-thick deposit. This result emphasizes that OR or WR motions provide better information in terms of settlement even

when significant site effects are expected. In Figures 5b and 5c, the efficiency of all IMs improved for profiles with liquefiable layers that are at the extremes (thin or deep). We expect small settlements in these cases (Karimi et al. 2018; Bullock et al. 2018a), so this trend in efficiency may reflect heteroscedasticity with regard to settlement (i.e., that uncertainty is smaller for smaller predicted settlements). Appendix D provides similar figures for $S_{S,M,P}$ and $S_{S,R,P}$, which were less sensitive to changes in the profile's geometry.

Appendix D provides similar figures for $E_{\theta,P}$ as a function of both profile geometry and foundation properties. Trends are not as apparent for predicting tilt, reflecting the increased uncertainty around numerical predictions of tilt as compared to settlement (Karimi and Dashti 2016b). Figure 6 shows that $S_{\theta,M,P}$ and $S_{\theta,R,P}$ are likewise insensitive to profile geometry and B. However, both are improved by increases in foundation bearing pressure (q) (Figure 6), which has a re-centering effect on tilt (Bullock et al. 2018b;2019). All IMs have improved $S_{\theta,M,P}$ and $S_{\theta,R,P}$ for larger q, which suggests that tilt may be less sensitive to ground motion intensity in general when q is larger. However, this finding does not suggest that any IM is superior based on sufficiency.

EFFICIENCY OF IMS FROM THE CENTRIFUGE TEST DATABASE

We next consider comprehensive efficiency in the centrifuge experimental database. Due to the limitations of centrifuge modeling discussed previously, we anticipate that results from later motions in a given test are more likely to be less useful because the structures and soil profile begin in a damaged or disturbed state. To address this bias, we replace Equation 2 with 8 for the analysis in this section to include a term for the sequence number of each given test, N_{seq} ($N_{seq} = 1$ for the first motion experienced by a given model). Further discussion of the selection of this metric for reliability is provided in Appendix E. Efficiency is subsequently calculated according to the methodology above.

$$\ln(DP) = a_0 + a_1 \ln\left(N_{seq}\right) + a_2 \ln(IM) + \varepsilon_{DP|IM} \quad 8$$

EFFICIENCY OF SINGLE IMS

Table 4 reports $E_{S,C}$ and $E_{\theta,C}$ of all IMs for transverse motions at the three locations described above, as well as the rotational motion at the foundation obtained from centrifuge recordings. In all cases, the OR or WR motion provided better $E_{DP,C}$ than any of the surficial locations

(transverse or rotational). This agrees with the findings from analysis of the numerical data in the previous section; outcropping rock motion is the best predictor of liquefaction consequences, perhaps because it reflects the total seismic excitation applied to the soil-foundation-structure system, rather than solely the excitation influenced by site response and soil softening or damping. Thus, other properties of soil and structure that are critical predictors of foundation's settlement or tilt must be considered separately in a predictive model, independent of the IM.

The hierarchy of performance among the IMs is similar for predicting foundation residual tilt in the centrifuge test database to that in the numerical database (Appendix A). Most IMs have very similar efficiency, with the exception of the significant durations, which perform worse. For settlement, the superior performance of the evolutionary IMs relative to the peak transient IMs is still apparent, with the exception of three peak transient IMs that had similar efficiency to the evolutionary IMs: $S_a(T_{so})$, $S_{a,avg}(0.2T_{so}, 1.5T_{so})$, and $S_a(0.2T_{so}, 2T_{so})$. This suggests that the frequency content of motion near the fundamental site period (both its initial and lengthened values) is more efficient for the centrifuge test results than for the numerical models. Although the numerical models capture softening in the liquefiable layers, they do not adequately capture the dilation cycles and the corresponding acceleration spikes at large shear strains over time (Karimi and Dashti 2015, 2016) nor the actual phase change behavior (i.e., solid-like to fluid-like, and vice versa) of liquefied sand observed in experiments. The shaking intensity rate (SIR) is also more efficient in the centrifuge results than in the numerical data for settlement.

EFFICIENCY OF VECTOR IMS

We extend this analysis to consider pairs of IMs. Figure 7 shows $E_{S,C}$ of select pairs of evolutionary and peak transient IMs. The efficiency of pairs of outcropping rock IMs is up to 20% better than the single IMs in the pair for predicting settlement. Generally, the benefits to efficiency for using a paired IM at other locations are marginal (0% to 5%) for predicting settlement, and likewise marginal at all locations for predicting residual tilt (figure provided in Appendix D). However, pairs of transverse foundation IMs including PGA and pairs of far-field motion IMs including CAV_{DP} benefit substantially (up to 15% improvement in $E_{S,C}$). Paired IMs in these two cases perform similarly to single or paired outcropping rock IMs for predicting settlement.

EFFICIENCY OF TRANSVERSE-ROTATIONAL IMS

Table 5 provides $E_{S,C}$ and $E_{\theta,C}$ for select pairs of one transverse foundation IM and one rotational foundation IM. Recall that transverse foundation IMs are calculated using the horizontal acceleration at the foundation, while rotational foundation IMs are calculated based on the rotational acceleration of the foundation about its centroid. These pairs generally have better $E_{S,C}$ than single foundation or far-field IMs, but are slightly less efficient than single or pairs of outcropping rock IMs. However, certain pairs offer the best $E_{\theta,C}$ of any IMs identified in this study. Specifically, transverse CAV paired with rotational CAV is 9% more efficient than any pair of one evolutionary and one peak transient IM measured on outcropping rock. Vector IMs including another evolutionary transverse IM or transverse V_{gi} are also relatively efficient.

PREDICTABILITY OF ALL INTENSITY MEASURES

AVAILABILITY AND UNCERTAINTY OF GROUND MOTION MODELS

Many of the IMs in this study can be directly predicted by GMMs (e.g., PGA, CAV, and D_{5-75}). However, others require additional effort (e.g., $S_{a,avg}$ and CAV_{DP}). Additionally, we must first develop correlation models in order to predict the joint occurrence of paired IMs. Such correlation models are only currently available for a limited set of IM pairs.

Table 6 provides a summary of the GMMs in the literature that predict the considered IMs directly. The lists provided are intended to be representative, but are certainly not exhaustive. GMMs for PGA, PGV, and S_a are plentiful in the literature. Broadly applicable models exist for the shallow crustal (e.g., Campbell and Bozorgnia 2014), subduction (e.g., Atkinson and Boore 2003), and intraplate tectonic environments (e.g., Darragh et al. 2015), and many models exist for use in specific regions (e.g., Bradley 2013). Models for certain non-spectral IMs are also becoming common and available for more contexts (e.g., Danciu and Tselentis 2007; Bullock et al. 2017). Although a handful of models currently exist for predicting the significant duration of motion (Kempton and Stewart 2006; Bommer et al. 2009; Afshari and Stewart 2016), they are at present limited to the shallow crustal tectonic environment.

Models for S_a can be extended and combined with correlation models to generate probabilistic predictions of $S_{a,avg}$, as discussed in Eads et al. (2015). Models exist for

estimating the correlation among S_a values at multiple periods (e.g., Baker and Bradley 2017), but only for the shallow crustal tectonic environment. This limits the practicality of using $S_{a,avg}$ in models for predicting liquefaction consequences in other environments. The same limitation will apply to vector IMs until correlation models are developed for the relevant non-spectral IMs and for more tectonic environments, although models for the correlation between S_a and significant duration exist for shallow crustal events (e.g., Baker and Bradley 2017).

Finally, no model exists for predicting SIR directly, but predictions of AI and significant duration can be combined to predict SIR. However, characterizing the uncertainty around these predictions would require quantifying the correlation between the errors in predicting each component.

PREDICTABILITY AS A FUNCTION OF THE DEFINITION OF MOTION

The definition and location of motion has major implications for the predictability of IMs. First, no GMM includes the effects of soil-structure interaction that influence foundation (transverse or rotational) motion, meaning that foundation IMs are impractical to predict without performing nonlinear 3D dynamic analyses of soil-foundation-structure systems using hazard-representative outcropping rock ground motion records as inputs. Predicting motion at the far-field surface (FF-EL) and within rock (WR) locations would require performing 1D equivalent-linear, total-stress site response analyses. However, some GMMs that used equivalent-linear analyses to constrain their site terms predict the FF-EL intensity directly (e.g., Walling et al. 2008; Seyhan and Stewart 2014). These analyses thereby necessitate knowledge of the density and shear wave velocity of the bedrock at the site, as well as the dynamic properties of the overlying soil profile.

GMMs that include site effects (typically as a function of the time-averaged shear wave velocity in the top 30 m of the site, $V_{S,30}$, and sometimes the depth to a layer with shear wave velocity of 1,000 m/s or 2,500 m/s, $Z_{1.0}$ or $Z_{2.5}$) are based on real ground motion recordings. Therefore, the site effects included are governed by potentially nonlinear, effective stress behavior, meaning that predictions made by GMMs including site effects most nearly approximate the FF-NL motion. However, these GMMs are typically only applicable to $V_{S,30}$ exceeding 180 m/s and assume that site effects can be described as a logarithmic function of $V_{S,30}$, neither of which may be valid for profiles with liquefiable materials (particularly those

with thick, loose deposits of saturated granular soils). GMMs that assume such simplified site effects are still based on ground motion records that include real nonlinear effects, meaning that these effects are reflected only in the model uncertainty. Some GMMs do include more complex, nonlinear site effects (e.g., Boore et al. 2014) or can be extended to do so (e.g., Seyhan and Stewart 2014), but these still do not explicitly predict the intensity at the surface above liquefied sand. Further, some profiles with liquefiable material will have $V_{S,30}$ less than 180 m/s, meaning that the functional forms of the GMMs may not yield reasonable estimates if the true profile $V_{S,30}$ is used as an input. Some GMMs predict outcropping rock motion specifically (e.g., Darragh et al. 2015; Bullock et al. 2017), although models including site effects can also approximate outcropping rock motion if the shear wave velocity of rock is used in place of $V_{S,30}$.

We conclude that the outcropping rock motion is more predictable than any of the other definitions for the site conditions of interest, although 1D equivalent-linear site response analyses are also routinely performed in practice. Nevertheless, other definitions require more information and extra analyses (either nonlinear 3D or equivalent-linear 1D simulations), or tenuous assumptions regarding the linearity of site behavior and the applicability of GMMs (nonlinear far-field), which would add to the underlying uncertainties.

CONCLUDING REMARKS

According to a comprehensive numerical database containing both 3D nonlinear simulations of soil-foundation-structure systems and 1D equivalent-linear site response analyses, outcropping rock CAV offers the optimum combination of efficiency, sufficiency, and predictability for predicting the permanent settlement of shallow-founded structures on liquefiable sites. Using a vector IM does not notably improve efficiency or sufficiency in predicting average settlement. Outcropping rock CAV, PGV, and V_{gi} are the optimum IMs for predicting foundation's residual tilt. However, a combination of two of these IMs may be preferable for tilt predictions, provided a correlation model for their prediction is developed.

Outcropping rock IMs may be better predictors of foundation settlement and tilt because they reflect the total seismic demand on the entire soil-foundation-structure system, rather than only the demand transferred to the foundation (i.e., transverse and rotational foundation IMs) or the ground surface (i.e., far-field IMs) that are the result of wave

propagation through a highly nonlinear and softened soil profile. In this sense, outcropping rock IMs influence not only the accelerations and pore pressures experienced throughout the soil column, but also soil-structure interaction and all volumetric and deviatoric mechanisms of deformation active below the foundation. Although IMs on the foundation were better predictors of foundation's ratcheting response, they did not perform as well in predicting all mechanisms contributing to foundation's cumulative settlement and rotation.

The available centrifuge experimental data involving mat-founded structures on liquefiable soils confirm the conclusions above, but also suggest that certain vector IMs may be particularly efficient (e.g., far-field CAV_{DP} and PGA for predicting settlement, and vector transverse-rotational foundation IMs for predicting residual tilt). The higher efficiency of vector transverse-rotational foundation IMs for predicting tilt show that foundation motion IMs are more closely tied to ratcheting-type deformations and are expected to have a stronger relative influence on tilt than on settlement. These vector IMs are currently less predictable than single outcropping rock IMs, however, and using outcropping rock IMs may therefore be preferable when developing predictive models for settlement and tilt (Bullock et al. 2018a,2019). The centrifuge database includes similar variation in ground motion intensity to that in the numerical database, but considerably less variation in soil-foundation-structure system parameters. In this sense, the results presented based on the centrifuge data serve to validate the conclusions based on the numerical data, while also elucidating the influence of rotational foundation motion.

Efficiency of IMs in predicting foundation's settlement improves for profile geometries where we expect small settlements (i.e., those with thinner or deeper layers of liquefiable material), which may reflect heteroscedasticity in settlement predictions. The same trend is not evident for residual tilt. However, the sufficiency of IMs with regard to both source distance and magnitude improves with increases in foundation bearing pressure, which has a re-centering effect on tilt. Tilt may therefore be less sensitive to ground motion intensity when bearing pressure is large. The hierarchy of IMs and their locations appears insensitive to the soil-foundation-structure parameters considered, which suggests that parametric efficiency and sufficiency do not influence IM selection for model development.

The conclusions summarized above are counterintuitive when considered in the context of many simplified procedures for liquefaction triggering that use the free-field surface cyclic

stress ratio (CSR) as the IM (e.g., Youd and Idriss 2001; Boulanger and Idriss 2014). Although it is not clear whether this IM was the most optimum choice for predicting liquefaction triggering (e.g., Kramer and Mitchell 2006), these procedures are based on observations of surficial manifestations of liquefaction away from the structure and therefore do not incorporate its influence on building performance. The existing body of literature for predicting liquefaction triggering in the free-field may not translate directly to the prediction of liquefaction consequences on shallow-founded structures (e.g., Karimi et al. 2018).

The relative efficiency of the outcropping rock motion may reflect the following distinction: surficial motion is predictive of surficial manifestations of liquefaction away from structures, but the rock seismic excitation input to the system is more predictive of the consequences for shallow-founded structures. Further research is needed to rule out the influence of numerical modeling choices (e.g., selection and calibration of soil constitutive models) on this conclusion, although past research suggests that this is not the case (e.g., Ramirez et al. 2018). Additionally, Kramer and Mitchell (2006) identified CAV_5 of the outcropping rock motion as an efficient, sufficient, and predictable IM for evaluating the liquefaction hazard in the free-field, thereby setting a precedent for using outcropping rock evolutionary IMs for predicting liquefaction and its consequences. For forward analysis, CSR may be somewhat impractical because it is often calculated from the PGA at the surface, which is not easily predictable in the presence of liquefiable sands, unless one ignores the generation of pore pressures and liquefaction through equivalent-linear analyses (as is commonly done in practice). Outcropping rock IMs are easily predictable for forward analysis (e.g., Bullock et al. 2017), but must typically also be estimated using GMMs for analysis of past scenarios. This limitation of outcropping rock IMs can be overcome by using the GMM's median prediction or by treating the IM value as a random variable with median and standard deviation provided by the GMM (e.g., Bullock et al. 2018a).

Karimi and Dashti (2017) and Dashti and Karimi (2017) likewise showed that cumulative absolute velocity (CAV) at the base of the soil column was the optimum IM for predicting settlement. This study corroborates that earlier finding using a larger database including both numerical and experimental results and with a larger variety of candidate IMs and IM locations. However, this study also identifies potential vector IMs for predicting settlement and extends this analysis to the prediction of residual tilt. The previous studies identified peak ground velocity (PGV) as the best predictor of rocking drift. This study also

identifies PGV as a useful IM for this purpose, but shows that peak incremental ground velocity (V_{gi}) – which was not previously considered – may perform better, and that either IM may be improved through combination with CAV. Further, this study confirms that outcropping rock IMs and within-rock IMs are nearly equivalent in their performance for the particular problem of interest, validating the use of outcropping rock IMs in the determination of hazard levels and selection of ground motions as inputs to analyses of liquefaction consequences on structures (e.g., Kramer and Mitchell 2006; Karimi et al. 2018). This finding has immediate utility for practitioners and researchers working to assess liquefaction consequences.

The main implications of this study for future development of models for predicting the consequences of liquefaction on shallow foundations are threefold: (1) models must clearly and carefully select a definition of "motion," because the efficiency, sufficiency, and predictability of IMs is very sensitive to this definition; (2) models using vector IMs should consider the additional uncertainty added due to correlation among IMs, which may counteract any benefits to efficiency and sufficiency; and (3) models using surficial IMs should consider how users will calculate those IMs, as well as whether those IMs fail to capture any effects of the total seismic excitation on the soil column. Bullock et al. (2018a) used outcropping rock CAV as the IM in a predictive model for foundation settlement on the basis of efficiency, sufficiency, and predictability, and Bullock et al. (2019) used outcropping rock CAV and V_{gi} as the IMs in a predictive model for foundation residual tilt. The latter selected IMs using cross validation, but the selections align with the findings of this study.

This study presents the most comprehensive analysis of the performance of various IMs for predicting foundation settlement and residual tilt on liquefiable sites to date. It identifies the optimum IMs for predicting both of these consequences given the current availability of ground motion models. The results highlight the importance of considering both predictive performance (efficiency and sufficiency) and predictability in IM selection when developing probabilistic models for the consequences of liquefaction on mat-founded structures. These findings are applicable only to structures on stiff mat foundations, and their applicability to other shallow foundation systems (e.g., isolated spread or strip foundations) is unknown.

ACKNOWLEDGMENTS

Support for this research was provided partly by the U.S. Department of Education under award number P200A150042, the U.S. National Science Foundation (NSF) through grant number

145431, and the Department of Civil, Environmental, and Architectural Engineering and the University of Colorado Boulder. Any opinions, findings, and conclusions expressed herein are those of the authors and do not necessarily reflect the views of the funding organizations. The numerical simulations utilized the Janus supercomputer, which is supported by the National Science Foundation (award number CNS-0821794) and the University of Colorado Boulder. The Janus supercomputer is a joint effort of the University of Colorado Boulder, the University of Colorado Denver, and the National Center for Atmospheric Research.

REFERENCES

Abrahamson, N. A., Silva, W. J., & Kamai, R. (2013). Update of the AS08 Ground-Motion Prediction equations based on the NGA-west2 data set. *Pacific Earthquake Engineering Research Center Report, 2013/04.*

Afshari, K., & Stewart, J. P. (2016). Physically parameterized prediction equations for significant duration in active crustal regions. *Earthquake Spectra*, *32*(4), 2057-2081.

Allmond, J. & Kutter, B. (2012). Centrifuge Testing of Rocking Foundations on Saturated and Submerged Sand: Centrifuge Data Report for JDA01. (Report No. UCD/CGMDR-12/01). University of California, Davis.

Allmond, J. & Kutter, B. (2013). Centrifuge Testing of Rocking Foundations on Saturated and Submerged Sand: Centrifuge Data Report for JDA02. (Report No. UCD/CGMDR-13/01). University of California, Davis.

Arias, A. (1970). A measure of earthquake intensity, in *Seismic Design for Nuclear Power Plants*, R. J. Hansen (Editor), The MIT Press, Cambridge, Massachusetts. 438–483.

Atkinson, G. M., & Boore, D. M. (2003). Empirical ground-motion relations for subduction-zone earthquakes and their application to Cascadia and other regions. *Bulletin of the Seismological Society of America*, *93*(4), 1703-1729.

Badanagki, M., Dashti, S**.,** Kirkwood, P. (2018). An Experimental Study of the Influence of Dense Granular Columns on the Performance of Level and Gently Sloping Liquefiable Sites. *ASCE Journal of Geotechnical and Geoenvironmental Engineering*, 144(9), https://doi.org/10.1061/(ASCE)GT.1943-5606.0001937.

Baker, J.W., & Bradley, B.A. (2017). Intensity measure correlations observed in the NGA-West2 database, and dependence of correlations on rupture and site parameters. *Earthquake Spectra*. *33*(1). 145-156.

Bianchini, M., Diotallevi, P. P., & Baker, J. W. (2009, September). Prediction of inelastic structural response using an average of spectral accelerations. In *Proc. of the 10th International Conference on Structural Safety and Reliability (ICOSSAR09)*, Osaka, Japan (pp. 13-17).

Bommer, J. J., Magenes, G., Hancock, J., & Penazzo, P. (2004). The influence of strong-motion duration on the seismic response of masonry structures. *Bulletin of Earthquake Engineering*, *2*(1), 1-26.

Bommer, J. J., & Martinez-Pereira, A. (1999). The effective duration of earthquake strong motion. *Journal of Earthquake Engineering*. *3*(02), 127-172.

Bommer, J. J., Stafford, P. J., & Alarcón, J. E. (2009). Empirical equations for the prediction of the significant, bracketed, and uniform duration of earthquake ground motion. *Bulletin of the Seismological Society of America*, *99*(6), 3217-3233.

Boore, D. M., Stewart, J. P., Seyhan, E., & Atkinson, G. M. (2014). NGA-West2 equations for predicting PGA, PGV, and 5% damped PSA for shallow crustal earthquakes. *Earthquake Spectra*, *30*(3), 1057-1085.

Boulanger, R.W. & Idriss, I. M. (2014). CPT and SPT based liquefaction triggering procedures. *Technical Report.* Rep. No. UCD/CGM-14, 1.

Bradley B.A. (2011). Correlation of significant duration with amplitude and cumulative intensity measures and its use in ground motion selection. *Journal of Earthquake Engineering. 15*(6). 809-832.

Bradley, B. A. (2013). A New Zealand-specific pseudospectral acceleration ground-motion prediction equation for active shallow crustal earthquakes based on foreign models. *Bulletin of the Seismological Society of America*, *103*(3), 1801-1822.

Bray, J. D., & Macedo, J. (2017). 6th Ishihara lecture: Simplified procedure for estimating liquefaction-induced building settlement. *Soil Dynamics and Earthquake Engineering*, *102*, 215-231.

Bray, J. D., & Travasarou, T. (2007). Simplified procedure for estimating earthquake-induced deviatoric slope displacements. *Journal of Geotechnical and Geoenvironmental Engineering*, 133(4), 381-392.

Bullock, Z., Dashti, S., Liel, A., Porter, K., Karimi, Z., & Bradley, B. (2017). Ground-Motion Prediction Equations for Arias Intensity, Cumulative Absolute Velocity, and Peak Incremental Ground Velocity for Rock Sites in Different Tectonic Environments. *Bulletin of the Seismological Society of America*, *107*(5), 2293-2309.

Bullock, Z., Karimi, Z., Dashti, S., Porter, K., Liel, A., & Franke, K. (2018a). A Physics-Informed Semi-Empirical Probabilistic Model for the Settlement of Shallow-Founded Structures on Liquefiable Ground. *Geotechnique*. Under review.

Bullock, Z., Karimi, Z., Dashti, S., Liel, A., & Porter, K. (2018b). Key Parameters for Predicting Residual Tilt of Shallow-Founded Structures Due to Liquefaction. In *Proceedings of Geotechnical Earthquake Engineering and Soil Dynamics V*. Austin, TX.

Bullock, Z., Dashti, S., Karimi, Z., Liel, A., Porter, K., & Franke, K. (2019). Probabilistic Models for Residual and Peak Transient Tilt of Mat-Founded Structures on Liquefiable Soils. *Journal of Geotechnical and Geoenvironmental Engineering*. 145(2).

Campbell, K. W., & Bozorgnia, Y. (2010). A comparison of ground motion prediction equations for Arias intensity and cumulative absolute velocity developed using a consistent database and functional form. *Earthquake Spectra*, *28*(3), 931-941.

Campbell, K. W., & Bozorgnia, Y. (2011). Prediction equations for the standardized version of cumulative absolute velocity as adapted for use in the shutdown of US nuclear power plants. *Nuclear Engineering and Design*, *241*(7), 2558-2569.

Campbell, K. W., & Bozorgnia, Y. (2014). NGA-West2 ground motion model for the average horizontal components of PGA, PGV, and 5% damped linear acceleration response spectra. *Earthquake Spectra*, *30*(3), 1087-1115.

738 Cetin, K. O., Bilge, H. T., Wu, J., Kammerer, A. M., & Seed, R. B. (2009). Probabilistic model for
739 the assessment of cyclically induced reconsolidation (volumetric) settlements. *Journal of*
740 *Geotechnical and Geoenvironmental Engineering*, 135(3), 387-398.

741 Chandramohan, R., Baker, J. W., & Deierlein, G. G. (2016). Quantifying the influence of ground
742 motion duration on structural collapse capacity using spectrally equivalent records. *Earthquake*
743 *Spectra*, *32*(2), 927-950.

744 Chiou, B. S. J., & Youngs, R. R. (2014). Update of the Chiou and Youngs NGA model for the
745 average horizontal component of peak ground motion and response spectra. *Earthquake Spectra*,
746 *30*(3), 1117-1153.

747 Cornell, C. A. (1968). Engineering seismic risk analysis. *Bulletin of the Seismological Society of*
748 *America*, *58*(5), 1583-1606.

749 Danciu, L., & Tselentis, G. A. (2007). Engineering ground-motion parameters attenuation
750 relationships for Greece. *Bulletin of the Seismological Society of America*, *97*(1B), 162-183.

751 Darendeli, B. M. (2001). Development of a new family of normalized modulus reduction and material
752 damping curves, *Ph. D. Dissertation*. University of Texas at Austin.

753 Darragh, R. B., Abrahamson, N. A., Silva, W. J., & Gregor, N. (2015). Development of hard rock
754 ground-motion models for Region 2 of central and eastern North America. *NGA-East: Median Ground-*
755 *Motion Models for the Central and Eastern North America Region*, 51-84. PEER.

756 Dashti, S. (2009). *Toward developing an engineering procedure for evaluating building performance*
757 *on softened ground.* PhD Dissertation. Department of Civil and Environmental Engineering, University
758 of California, Berkeley.

759 Dashti, S., Bray, J. D., Pestana, J. M., Riemer, M. R. & Wilson, D. (2010a). Centrifuge testing to
760 evaluate and mitigate liquefaction induced building settlement mechanisms. *Journal of Geotechnical*
761 *and Geoenvironmental Engineering*, 136(7), 918–929.

762 Dashti, S., Bray, J. D., Pestana, J. M., Riemer, M. R. & Wilson, D. (2010b). Mechanisms of
763 seismically-induced settlement of buildings with shallow foundations on liquefiable soil. *Journal of*
764 *Geotechnical and Geoenvironmental Engineering*, 136(1), 151–164.`

765 De Biasio, M., Grange, S., Dufour, F., Allain, F., & Petre-Lazar, I. (2014). A simple and efficient
766 intensity measure to account for nonlinear structural behavior. *Earthquake Spectra*, *30*(4), 1403-1426.

767 Eads, L., Miranda, E., & Lignos, D. G. (2015). Average spectral acceleration as an intensity measure
768 for collapse risk assessment. *Earthquake Engineering & Structural Dynamics*, *44*(12), 2057-2073.

769 Electric Power Research Institute. (2006). Program on technology innovation: 560 Use of cumulative
770 absolute velocity (CAV) in determining effects of small magnitude earthquakes on seismic hazard
771 analyses. *EPRI, Palo Alto, CA, and the US Department of Energy, Germantown, MD. 1014099.*

772 Elgamal, A., Yang, Z. & Parra, E. (2002). Computational modeling of cyclic mobility and post-
773 liquefaction site response. *Soil Dynamics and Earthquake Engineering* 22(4), 259–271.

774 Fiegel, G. L., & Kutter, B. L. (1994). Liquefaction mechanism for layered soils. *Journal of*
775 *geotechnical Engineering*, *120*(4), 737-755.

776 Field, E. H., Biasi, G. P., Bird, P., Dawson, T. E., Felzer, K. R., Jackson, D. D., Johnson, K. M.,
777 Jordan, T. H., Madden, C., Michael, A. J., & Milner, K. R. (2015). Long-term time-dependent
778 probabilities for the third Uniform California Earthquake Rupture Forecast (UCERF3). *Bulletin of the*
779 *Seismological Society of America*, *105*(2A), 511-543.

Foulser-Piggott, R., & Goda, K. (2015). Ground-Motion Prediction Models for Arias Intensity and Cumulative Absolute Velocity for Japanese Earthquakes Considering Single-Station Sigma and Within-Event Spatial Correlation. *Bulletin of the Seismological Society of America*, *105*(4), 1903-1918.

Hashash, Y.M.A., Musgrove, M.I., Harmon, J.A., Groholski, D.R., Phillips, C.A., Park, D. (2016). DEEPSOIL 6.1, User Manual. *Board of Trustees of Univ. of Ill. at Urbana-Cham.*. Urbana, IL.

Jamiolkowski, M., Leroueil, S., Lo Presti, D. C. F. (1991). Theme lecture: Design parameters from theory to practice. *Proceedings, Geo-Coast*. *91*. 1-41.

Jampole, E., Deierlein, G., Miranda, E., Fell, B., Swensen, S., & Acevedo, C. (2016). Full-Scale Dynamic Testing of a Sliding Seismically Isolated Unibody House. *Earthquake Spectra*, *32*(4), 2245-2270.

Karimi, Z. & Dashti, S. (2015). Numerical and centrifuge modeling of seismic soil-foundation-structure interaction on liquefiable ground. *J. Geotech. Geoenviron. Eng.* 142(1), 04015061.

Karimi, Z. & Dashti, S. (2016). Seismic performance of shallow founded structures on liquefiable ground: Validation of numerical simulations using centrifuge experiments. *J. Geotech. Geoenviron. Eng.* 142(6), 04016011.

Karimi, Z. & Dashti, S. (2017). Ground motion intensity measures to evaluate II: the performance of shallow-founded structures on liquefiable ground. *Earthquake Spectra* 33(1), 277–298.

Karimi, Z., Dashti, S., Bullock, Z., Porter, K. & Liel, A. (2018). Key predictors of structure settlement on liquefiable ground: A numerical parametric study. *Soil Dynamics and Earthquake Engineering* In press.

Kayen, R. E., & Mitchell, J. K. (1997). Assessment of liquefaction potential during earthquakes by Arias intensity. *Journal of Geotechnical and Geoenvironmental Engineering*, *123*(12), 1162-1174.

Kempton, J. J., & Stewart, J. P. (2006). Prediction equations for significant duration of earthquake ground motions considering site and near-source effects. *Earthquake Spectra*, *22*(4), 985-1013.

Kramer, S. L. (1996). Geotechnical Earthquake Engineering. *Prentice Hall*. New York.

Kramer, S. L., Mitchell, R. A. (2006). Ground motion intensity measures for liquefaction hazard evaluation. *Earthquake Spectra*, *22*(2). 413-438.

Lysmer, J., Kuhlemeyer, R. L. (1969). Finite dynamic model for infinite media. *Journal of the Engineering Mechanics Division. 95*(4). 859-877.

Mason, H. B., Trombetta, N. W., Chen, Z., Bray, J. D., Hutchinson, T. C., & Kutter, B. L. (2013). Seismic soil–foundation–structure interaction observed in geotechnical centrifuge experiments. *Soil Dynamics and Earthquake Engineering*, 48, 162-174.

Olarte, J. C., Dashti, S., Liel, A. B., & Paramasivam, B. (2018). Effects of drainage control on densification as a liquefaction mitigation technique. *Soil Dynamics and Earthquake Engineering*, 110, 212-231.

Olarte, J., Paramasivam, B., Dashti, S., Liel, L. & Zannin, J. (2017). Centrifuge modeling of mitigation-soil-foundation-structure interaction on liquefiable ground. *Soil Dynamics and Earthquake Engineering* 97, 304–323.

Padgett, J. E., Nielson, B. G., & DesRoches, R. (2008). Selection of optimal intensity measures in probabilistic seismic demand models of highway bridge portfolios. *Earthquake Engineering & Structural Dynamics*, *37*(5), 711-725.

Paramasivam, B., Dashti, S., Liel, A. B., & Olarte, J. C. (2018a). Centrifuge modelling of mitigation-soil-structure-interaction on layered liquefiable soil deposits with a silt cap. In *Physical Modelling in Geotechnics, Volume 2* (pp. 1005-1010). CRC Press.

Paramasivam, B., Dashti, S.**,** Liel, A. (2018b). Impact of Spatial Variations in Permeability of Liquefiable Deposits on the Seismic Performance of Structures and Effectiveness of Drains," *ASCE Journal of Geotechnical and Geoenvironmental Engineering*, Accepted.

Paramasivam, B., Dashti, S. & Liel, A. B. (2017). Influence of prefabricated vertical drains on the seismic performance of structures founded on liquefiable soils. *Journal of Geotechnical and Geoenvironmental Engineering.* In Press.

Raghunandan, M., & Liel, A. B. (2013). Effect of ground motion duration on earthquake-induced structural collapse. *Structural Safety*, *41*, 119-133.

Ramirez, J., Barrero, A. R., Chen, L., Dashti, S., Ghofrani, A., Taiebat, M., & Arduino, P. (2018). Site response in a layered liquefiable deposit: evaluation of different numerical tools and methodologies with centrifuge experimental results. *Journal of Geotechnical and Geoenvironmental Engineering*, 144(10), 04018073.

Seyhan, E., & Stewart, J. P. (2014). Semi-empirical nonlinear site amplification from NGA-West2 data and simulations. *Earthquake Spectra, 30*(3), 1241-1256.

Shome N., Cornell C.A., 1999, Probabilistic seismic demand analysis of nonlinear structures, Reliability of Marine Structures Program Report No. RMS-35, Department of Civil and Environmental Engineering, Stanford University, California.

Stafford, P. J., Berrill, J. B., & Pettinga, J. R. (2009). New predictive equations for Arias intensity from crustal earthquakes in New Zealand. *Journal of Seismology*, *13*(1), 31-52.

Stewart, J. P., Afshari, K., & Hashash, Y. M. (2014). Guidelines for performing hazard-consistent one-dimensional ground response analysis for ground motion prediction. *PEER Report 2014, 16*. Pacific Earthquake Engineering Research Center, University of California, Berkeley. Berkeley, CA.

Travasarou, T., Bray, J. D., & Abrahamson, N. A. (2003). Empirical attenuation relationship for Arias intensity. *Earthquake Engineering & Structural Dynamics*, *32*(7), 1133-1155.

Trombetta, N. W., Mason, H. B., Chen, Z., Hutchinson, T. C., Bray, J. D., & Kutter, B. L. (2013). Nonlinear dynamic foundation and frame structure response observed in geotechnical centrifuge experiments. *Soil Dynamics and Earthquake Engineering*, 50, 117-133.

Unutmaz, B. & Cetin, K. O. (2012). Post-cyclic settlement and tilting potential of mat foundations. *Soil Dynamics and Earthquake Engineering*, 43, 271–286.

Walling, M., Silva, W., & Abrahamson, N. (2008). Nonlinear site amplification factors for constraining the NGA models. *Earthquake Spectra*, *24*(1), 243-255.

Youd, T. L. & Idriss, I. M. (2001). Liquefaction resistance of soils: summary report from the 1996 NCEER and 1998 NCEER /NSF workshops on evaluation of liquefaction resistance of soils. *Journal of Geotechnical and Geoenvironmental Engineering* 127(10), 817–833.

860 **Table 1.** Summary of the centrifuge experimental database.

Reference	Number of data points
Allmond and Kutter (2012, 2013)	74
Dashti et al. (2010a,b)	18
Olarte et al. (2017)	10
Paramasivam et al. (2017)	3

861

862

Table 2. Intensity measures considered in this study.

Type	IM	Equation	Reference
PT[a)]	PGA	$PGA = \max(\lvert a(t) \rvert)$	-
PT	PGV	$PGV = \max\left\lvert\left(\int_0^t a(t)dt\right)\right\rvert$	-
PT	V_{gi}	$V_{gi} = \max_i\left(\int_{t_{i1}}^{t_{i2}} \lvert a(t) \rvert dt\right)$	Jampole et al. 2016
PT	$S_a(1.0)$	-	-
PT	$S_a(T_{st})$	-	-
PT	$S_a(T_{so})$	-	-
PT	$S_a(1.5T_{so})$	-	-
PT	$S_a(2T_{so})$	-	-
PT	$S_{a,avg}(0.2T_{st}, 3T_{st})$	$S_{a,avg}(0.2T_{st}, 3T_{st}) = \left(\prod_{i=1}^{N} S_a(T = T_i)\right)^{1/N}$	Eads et al. 2015
PT	$S_{a,avg}(0.2T_{so}, 1.5T_{so})$	$S_{a,avg}(0.2T_{so}, 1.5T_{so}) = \left(\prod_{i=1}^{N} S_a(T = T_i)\right)^{1/N}$	-
PT	$S_{a,avg}(0.2T_{so}, 2T_{so})$	$S_{a,avg}(0.2T_{so}, 2T_{so}) = \left(\prod_{i=1}^{N} S_a(T = T_i)\right)^{1/N}$	-
EV[b)]	CAV	$CAV = \int_0^{t_d} \lvert a(t) \rvert dt$	EPRI 1998
EV	CAV_5	$CAV_5 = \int_0^{t_d} \chi\langle a(t) \rangle \lvert a(t) \rvert dt$[b)]	Kramer and Mitchell 2006
EV	CAV_{STD}	$CAV_{STD} = \sum_{i=1}^{t_d}\left(H(PGA_i - 0.025)\int_{i-1}^{i} \lvert a(t) \rvert dt\right)$[b)]	EPRI 2006
EV	CAV_{DP}	-	Campbell and Bozorgnia 2011
EV	AI	$AI = \frac{\pi}{2g}\int_0^{t_d} a(t)^2 dt$	Arias 1970
DR[c)]	D_{5-75}	-	Bommer and Martinez-Pereira 1999
DR	D_{5-95}	-	Bommer and Martinez-Pereira 1999
DR	SIR_{75}	$SIR_{75} = \frac{0.7AI}{D_{5-75}}$	Dashti et al. 2010a
DR	SIR_{95}	$SIR_{95} = \frac{0.9AI}{D_{5-75}}$	Dashti et al. 2010a

a) Peak transient; b) Evolutionary; c) Duration-related

b) $\chi\langle\cdot\rangle$: a filter that is zero when the argument is below 5 cm/s^2; $H(\cdot)$: the Heaviside step function.

868 **Table 3.** Comprehensive efficiency ($E_{S,C}$) and sufficiency with respect to magnitude and distance-to-
869 rupture ($S_{S,M,C}$ and $S_{S,R,C}$) of selected pairs of outcropping rock IMs, as compared to the values for
870 each individual IM, for predicting settlement. The columns for either "IM_1" or "IM_2" report values
871 calculated using only that IM, while the columns for "IM_1 and IM_2" use both IMs.

IM_1	IM_2	$E_{S,C}$			$S_{S,M,C}$			$S_{S,R,C}$		
		IM_1	IM_2	IM_1 and IM_2	IM_1	IM_2	IM_1 and IM_2	IM_1	IM_2	IM_1 and IM_2
CAV	PGA	0.68	0.81	0.68	0.00	0.31	0.02	0.11	0.03	0.01
CAV	V_{gi}	0.68	0.76	0.66	0.00	0.24	0.03	0.11	0.11	0.02
CAV	$S_a(1.0)$	0.68	0.78	0.66	0.00	0.23	0.02	0.11	0.09	0.01
CAV	$S_{a,avg}(0.2T_{so}, 2T_{so})$	0.68	0.77	0.66	0.00	0.28	0.04	0.11	0.08	0.04
D_{5-75}	PGA	0.90	0.81	0.72	0.27	0.31	0.06	0.33	0.03	0.06
D_{5-75}	V_{gi}	0.90	0.76	0.70	0.27	0.24	0.06	0.33	0.11	0.02
D_{5-75}	$S_a(1.0)$	0.90	0.78	0.75	0.27	0.23	0.11	0.33	0.09	0.06
D_{5-75}	$S_{a,avg}(0.2T_{so}, 2T_{so})$	0.90	0.77	0.69	0.27	0.28	0.06	0.33	0.08	0.04

872

873

Table 4. Comprehensive efficiency for all IMs at all locations for predicting foundation settlement ($E_{S,C}$) and residual tilt ($E_{\theta,C}$) for the centrifuge test results. All IMs for the outcropping rock, far-field surface, and transverse foundation accelerations are calculated based on recorded horizontal accelerations, while the IMs for the rotational foundation acceleration are calculated based on recorded rotational accelerations around the foundation centroid.

IM	**Outcropping rock**		**Far-field**		**Foundation (transverse)**		**Foundation (rotational)**	
	$E_{S,C}$	$E_{\theta,C}$	$E_{S,C}$	$E_{\theta,C}$	$E_{S,C}$	$E_{\theta,C}$	$E_{S,C}$	$E_{\theta,C}$
CAV	0.57	0.97	0.80	1.22	0.64	1.10	0.73	1.19
CAV_5	0.52	0.96	0.76	1.14	0.64	1.11	-	-
CAV_{STD}	0.53	0.97	0.80	1.17	0.65	1.11	-	-
CAV_{DP}	0.50	0.96	0.68	1.19	0.68	1.10	-	-
AI	0.45	0.95	0.80	1.21	0.65	1.11	-	-
PGA	0.46	0.95	0.78	1.15	0.58	1.07	0.73	1.13
PGV	0.79	1.15	0.81	1.22	0.70	1.13	0.80	1.23
V_{gi}	0.57	1.02	0.80	1.22	0.70	1.17	0.72	1.16
$S_a(1.0)$	0.50	0.98	0.81	1.20	0.68	1.09	0.80	1.18
$S_a(T_{st})$	0.56	1.05	0.79	1.17	0.66	1.03	0.77	1.16
$S_a(T_{so})$	0.45	0.97	0.79	1.17	0.68	1.07	0.67	1.05
$S_a(1.5T_{so})$	0.52	1.03	0.79	1.18	0.65	1.05	0.67	0.99
$S_a(2T_{so})$	0.50	1.01	0.80	1.19	0.69	1.14	0.77	1.13
$S_{a,avg}(0.2T_{st}, 3T_{st})$	0.61	1.08	0.78	1.17	0.62	1.04	0.67	1.00
$S_{a,avg}(0.2T_{so}, 1.5T_{so})$	0.44	0.98	0.79	1.16	0.63	1.05	0.66	1.05
$S_{a,avg}(0.2T_{so}, 2T_{so})$	0.45	0.98	0.79	1.17	0.64	1.07	0.68	1.06
D_{5-75}	0.83	1.22	0.82	1.20	0.82	1.20	-	-
D_{5-95}	0.80	1.22	0.82	1.20	0.81	1.21	-	-
SIR_{75}	0.46	0.98	0.80	1.20	0.70	1.16	-	-
SIR_{95}	0.52	1.02	0.80	1.20	0.73	1.17	-	-

Table 5. Comprehensive efficiency for pairs of transverse and rotational foundation motion IMs for predicting foundation settlement and residual tilt for the centrifuge test results. The columns for either "IM_1" or "IM_2" report values calculated using only that IM (i.e., only a transverse or a rotational IM), while the columns for "IM_1 and IM_2" use both IMs.

Transverse IM (IM_1)	**Rotational IM (IM_2)**	$E_{S,C}$			$E_{\theta,C}$		
		IM_1	IM_2	IM_1 and IM_2	IM_1	IM_2	IM_1 and IM_2
CAV	CAV	0.64	0.73	0.63	1.10	1.19	0.86
CAV	PGA	0.64	0.73	0.63	1.10	1.13	0.92
V_{gi}	CAV	0.70	0.73	0.58	1.17	1.19	0.95
V_{gi}	PGA	0.70	0.73	0.61	1.17	1.13	0.94
PGA	CAV	0.58	0.73	0.60	1.07	1.19	1.05

Table 6. Model availability and prediction uncertainty for IMs which can be predicted directly by GMMs.

IM	Models	Tectonic environments	Prediction uncertainty (σ_p)
CAV	Danciu and Tselentis (2007), Campbell and Bozorgnia (2010), Foulser-Piggott and Goda (2015), Bullock et al. (2017)	C[1], S[2], I[3]	0.4 to 0.7
CAV_5	Kramer and Mitchell (2006), Danciu and Tselentis (2007), Bullock et al. (2017)	C, S, I	0.7 to 0.9
CAV_{STD}	Bullock et al. (2017)	C, S, I	0.5 to 0.7
CAV_{STD}	Campbell and Bozorgnia (2011)	C	0.6
AI	Travasarou et al. (2003), Danciu and Tselentis (2007), Stafford et al. (2009), Foulser-Piggott and Goda (2015), Bullock et al. (2017)	C, S, I	1.0 to 1.4
PGA, $S_a(T)$	Atkinson and Boore (2003), Boore et al. (2014), Abrahamson et al. (2013), Campbell and Bozorgnia (2014), Chiou and Youngs (2014), Darragh et al. (2015)	C, S, I	0.3 to 0.8
PGV	Atkinson and Boore (2003), Danciu and Tselentis (2007), Abrahamson et al. (2013), Boore et al. (2014), Campbell and Bozorgnia (2014), Chiou and Youngs (2014), Darragh et al. (2015)	C, S, I	0.5 to 0.8
V_{gi}	Bullock et al. (2017)	C, S, I	0.5 to 0.7
D_{5-75}, D_{5-95}	Kempton and Stewart (2006), Bommer et al. (2009), Afshari and Stewart (2016)	C	0.3 to 0.8

[1]Shallow crustal; [2]Subduction; [3]Intraplate

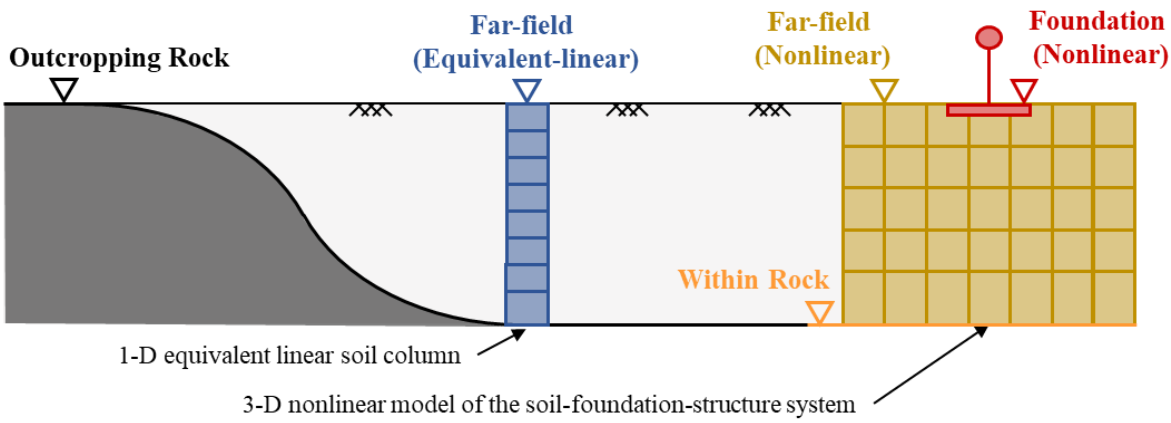

894

895 **Figure 1.** Schematic view of the locations considered when defining the motion.

896

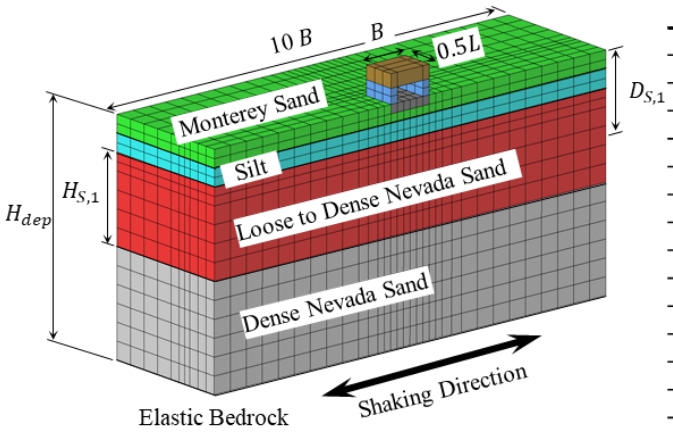

Parameter	Range
Relative density	30% to 85%
Thickness of susc. Layer, $H_{S,1}$	1m to 20m
Depth to middle of susc. layer, $D_{S,1}$	0m to 10m
Number of susc. layers	1 to 3
Low permeability cap	Present or absent
Deposit depth, H_{Dep}	12m to 80m
Bearing pressure	39kPa to 220kPa
Foundation embedment depth	1m to 5m
Foundation width, B	4.5m to 15m
Foundation L/B ratio	1.0 to 10.0
Structure H/B ratio	0.3 to 2.3
Structure height	2.6m to 13.7m
Structure mass	5 tons to 2,472 tons
Structure period	0.25s to 2.0s
Bedrock shear wave velocity	760m/s to 2000m/s

Figure 2. Schematic of numerical model (Karimi et al. 2018) and summary table of parameters that were varied in numerical dataset used here.

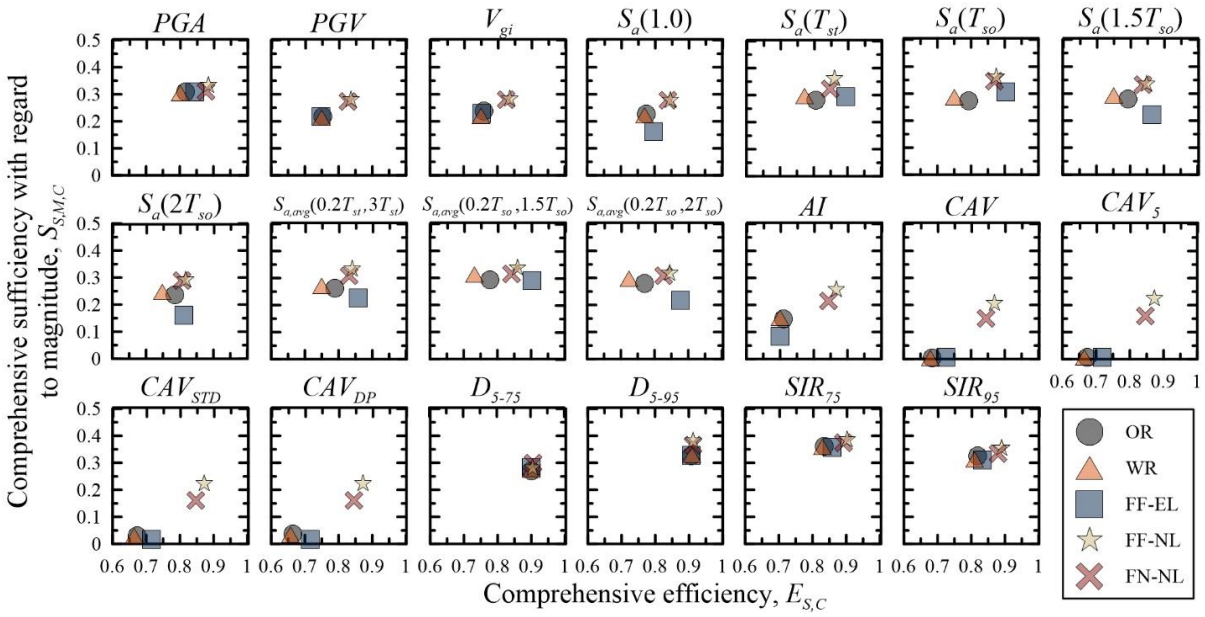

Figure 3. Comprehensive efficiency and sufficiency with regard to magnitude for all IMs for predicting foundation settlement, based on the numerical database. IMs at all locations are included: outcropping rock (OR), within-rock (WR), far-field calculated using equivalent-linear analyses (FF-EL), far-field calculated using nonlinear analyses (FF-NL), and foundation (FN-NL). Different shapes are used for peak transient, evolutionary, and duration-related IMs; different colors reflect different locations.

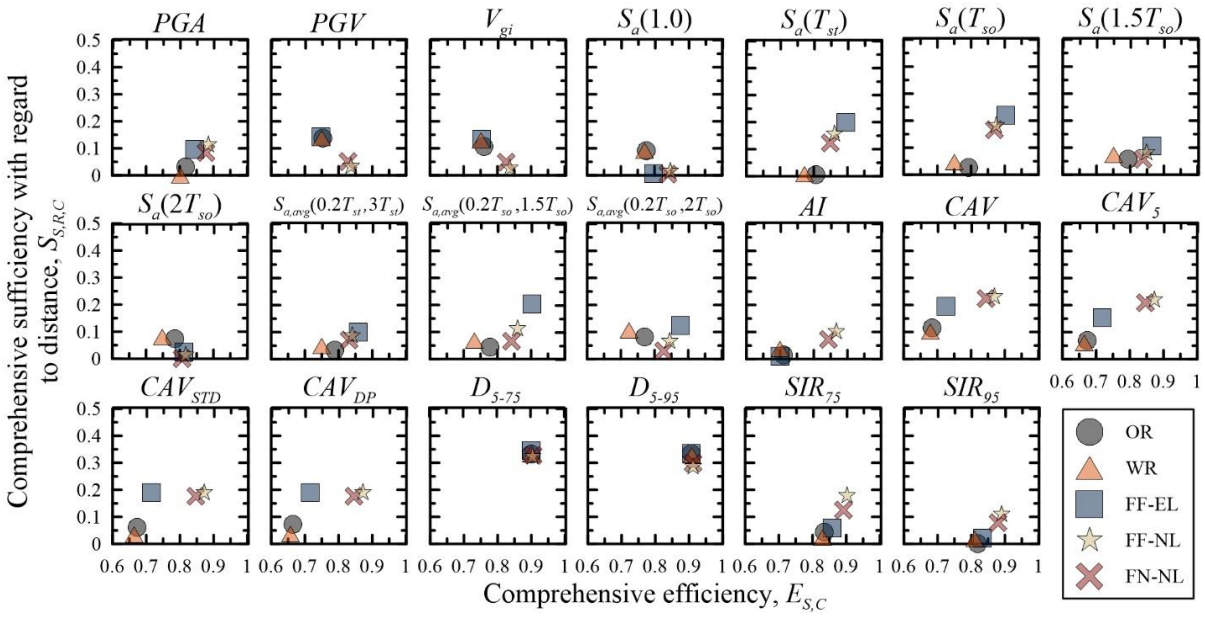

Figure 4. Comprehensive efficiency and sufficiency with regard to distance for all IMs for predicting foundation settlement, based on the numerical database. IMs at all locations are included: outcropping rock (OR), within-rock (WR), far-field calculated using equivalent-linear analyses (FF-EL), far-field calculated using nonlinear analyses (FF-NL), and foundation (FN-NL). Different shapes are used for peak transient, evolutionary, and duration-related IMs; different colors reflect different locations.

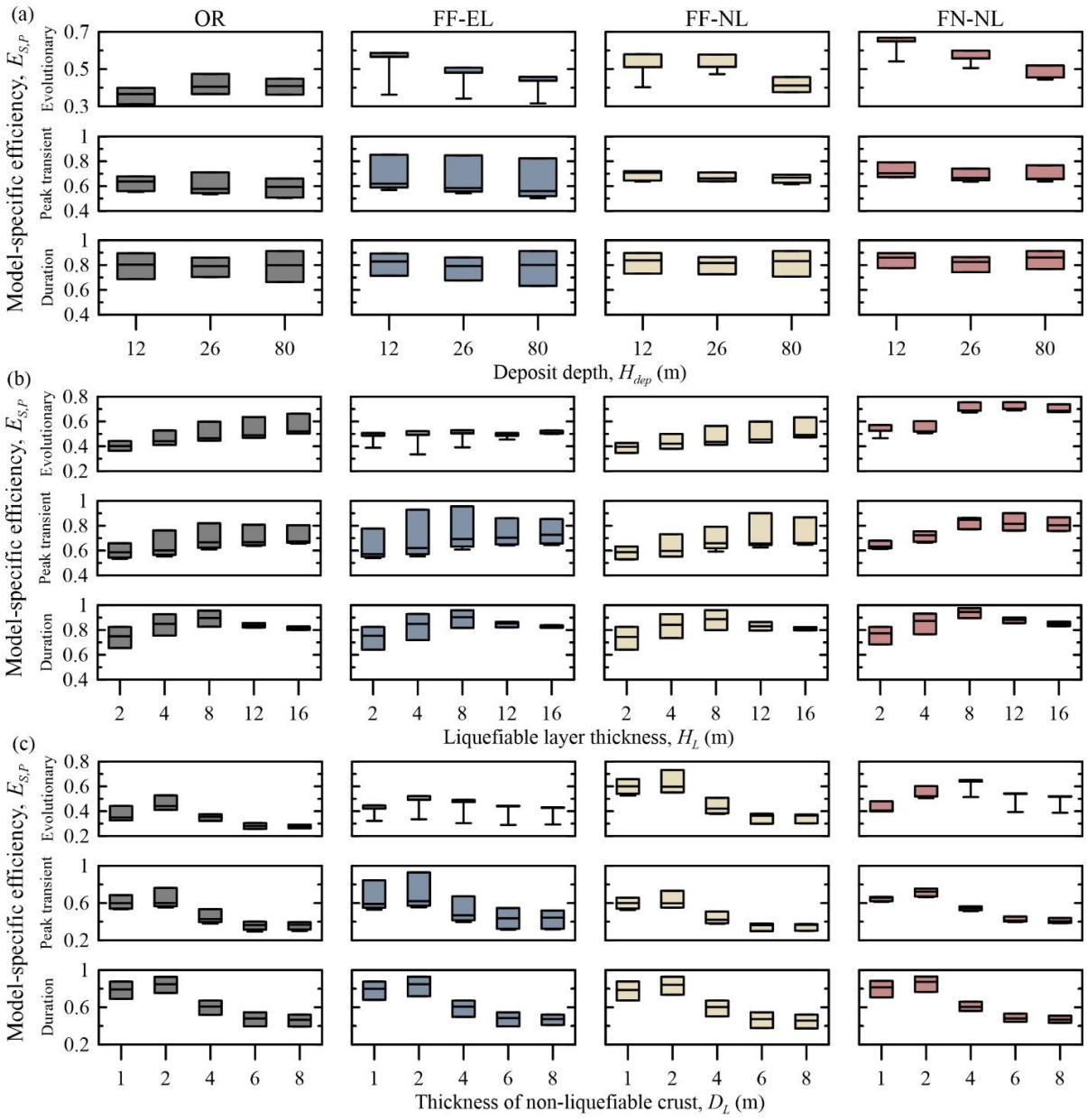

Figure 5. Parametric efficiency as a function of deposit depth, liquefiable layer thickness, and non-liquefiable crust thickness for all IMs for predicting foundation settlement, based on the numerical database. IMs at select locations are included: outcropping rock (OR), far-field calculated using equivalent-linear analyses (FF-EL), far-field calculated using nonlinear analyses (FF-NL), and foundation (FN-NL).

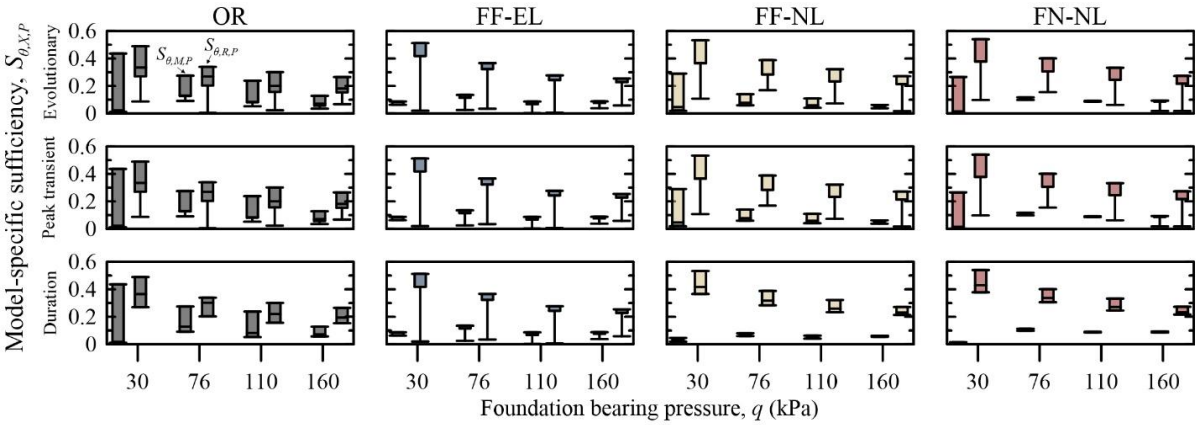

926

927 **Figure 6.** Parametric sufficiency with regard to both magnitude (left) and distance (right) as a
928 function of bearing pressure for all IMs at select locations for predicting residual tilt, based on the
929 numerical database. IMs at select locations are included: outcropping rock (OR), far-field calculated
930 using equivalent-linear analyses (FF-EL), far-field calculated using nonlinear analyses (FF-NL), and
931 foundation (FN-NL).
932

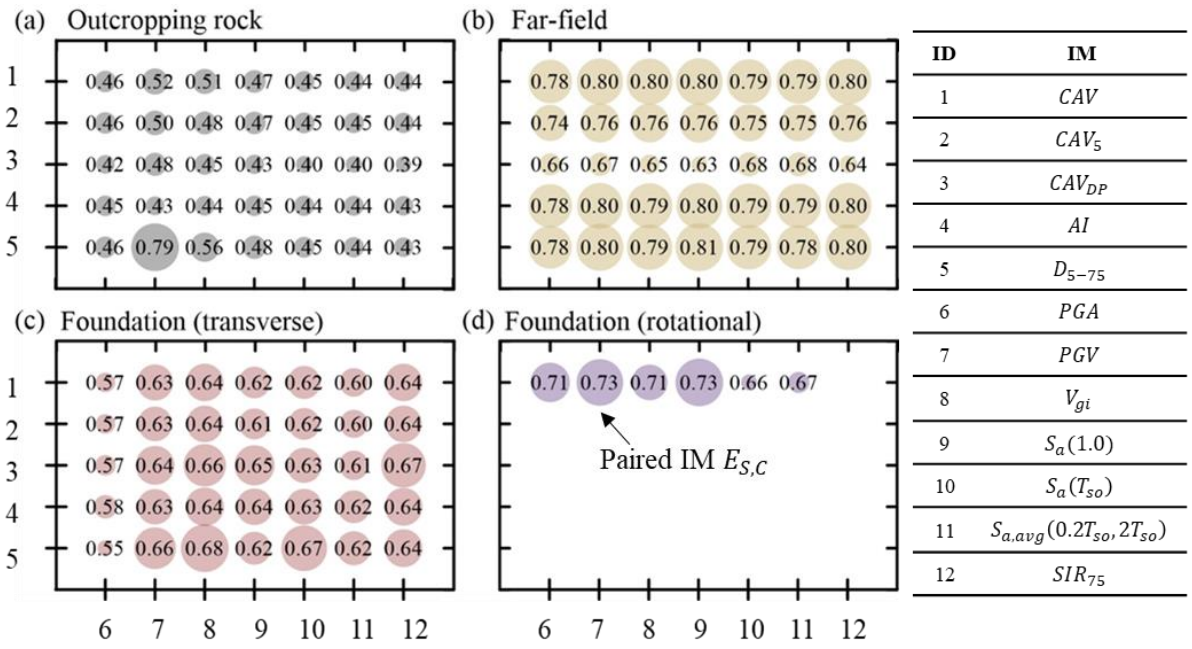

ID	IM
1	CAV
2	CAV_5
3	CAV_{DP}
4	AI
5	D_{5-75}
6	PGA
7	PGV
8	V_{gi}
9	$S_a(1.0)$
10	$S_a(T_{so})$
11	$S_{a,avg}(0.2T_{so}, 2T_{so})$
12	SIR_{75}

933

934 **Figure 7.** Comprehensive efficiency for select paired IMs at all locations for predicting foundation
935 settlement based on the centrifuge test results.